

# Varied Perturbation Theory for the Dispersion Dip in the Two-Dimensional Heisenberg Quantum Antiferromagnet

Götz S. Uhrig\*

*Lehrstuhl für Theoretische Physik I, Technische Universität Dortmund,  
Otto-Hahn Straße 4, 44221 Dortmund, Germany*

Kingshuk Majumdar

*Department of Physics, Grand Valley State University, Allendale, Michigan 49401, USA<sup>†</sup>*

(Dated: September 13, 2018)

We study the roton-like dip in the magnon dispersion at the boundary of the Brillouin zone in the isotropic  $S = 1/2$  Heisenberg quantum antiferromagnet. This high-energy feature is sometimes seen as indication of a fractionalization of the magnons to spinons. In this article, we provide evidence that the description of the dip in terms of magnons can be improved significantly by applying more advanced evaluation schemes. In particular, we illustrate the usefulness of the application of the principle of minimal sensitivity in varied perturbation theory. Thereby, we provide an example for the application of this approach to an extended condensed matter problem governed by correlations which can trigger analogous investigations for many other systems.

PACS numbers: 75.10.Jm, 75.30.Ds, 02.30.Mv, 75.50.Ee

## I. INTRODUCTION

Quantum antiferromagnetism is a long-standing issue which cannot be reviewed briefly, but see for instance Ref. 1. Yet there are still important aspects which are not clear. In particular, the dynamics at high energies is not yet fully understood. But the quantitative understanding of the high-energy dynamics is of increasing experimental relevance. For instance, the dispersion of spin waves in the two-dimensional parent compounds of the high-temperature superconductors displays dips which can only be accounted for by considering subdominant exchange couplings as well, for references and further discussion see Ref. 2. The relevance of the magnetic dynamics in the total Brillouin zone including the high-energy behavior close to the Brillouin zone boundary has recently been emphasized by inelastic X-ray scattering for doped and undoped cuprates<sup>3</sup>.

The purpose of the present article is partly methodological. Thus we discuss the fundamental system, namely the isotropic Heisenberg quantum antiferromagnet with spin  $S = 1/2$  and nearest neighbor exchange  $J > 0$

$$H = \frac{1}{2}J \sum_{i,\delta} \mathbf{S}_i \cdot \mathbf{S}_{i+\delta}, \quad (1)$$

where the subscript  $i$  runs over all sites and  $\delta$  runs over the vectors to the adjacent sites. This model is very well studied. But we focus on the roton-like dip at the wave vector  $\mathbf{k} = (\pi, 0)$  and its equivalent values (the lattice spacing is set to unity). This feature represents an open issue because it eludes precise calculation within spin wave theory.

On the one hand, the dispersion  $\omega(\mathbf{k})/S$  at  $\mathbf{k} = (\pi, 0)$  and at  $\mathbf{k} = (\pi/2, \pi/2)$  takes precisely the same value in linear spin wave theory which represents the leading

order in an expansion in  $1/S$ , where  $S$  is the spin value. In the next-leading, first order this remains true as well. On the other hand, series expansion for  $S = 1/2$  around the Ising limit predicts a dip of 8.6%<sup>4,5</sup> which is confirmed by quantum Monte Carlo with a dip of 9.6%<sup>6</sup>.

The idea suggests itself that further corrections of spin wave theory in  $1/S$  cure the above discrepancy<sup>7-9</sup>. But this seems not to be the case. Although in second order  $1/S^2$ , a small dip appears, it takes only 1.4% which is far from what one would like to have<sup>10</sup>. This number improves by about a factor of 2 upon passing to the third order  $1/S^3$  to 3.2%. But this is still far from the series and quantum Monte Carlo result<sup>10</sup>. The convergence turns out to be particularly slow.

One may view this observation as a mere mathematical problem. But one may also wonder why the convergence is so slow and come to the conclusion that the underlying physical description in terms of spin waves, also called magnons, is not appropriate and that the true nature of the elementary excitations is a different one, for instance that the magnons disintegrate to spinons. Such a view is indeed discussed in the interpretation of the experimental findings<sup>11-14</sup>. In Ref. 13 the dip is given to be 7(1)% analysing the experimental data. The naive analysis of the peak positions in Figs. 3a and 3b in Ref. 13 suggests even about 10% for the dip. In any case, a sizable dip is an experimentally well-supported fact.

Concerning the issue of the elementary excitations, it is useful to recall a well-studied system where the same question was discussed. In Heisenberg  $S = 1/2$  ladders with two legs the elementary excitations are  $S = 1$  triplons because no long-range order occurs. But multi-particle continua are sizeable as well<sup>15,16</sup> and they may be taken as precursors of a fractionalization towards spinons<sup>15</sup>. Interestingly, the important multi-particle continua and their energetic vicinity to the dispersion of

the elementary triplons<sup>16</sup> induces a dip in their dispersion at  $k = 0$  compared to  $k = \pi/2$ . But high order perturbative results are necessary to capture this effect<sup>15,17,18</sup>.

These observations led us to look for a quantitative description of the dip in the dispersion on the square lattice in terms of magnons. Since standard perturbation theory seems to be not particularly efficient, see above, we follow a modified approach. The basic idea is to stick essentially to a second order perturbative approach, but to vary the starting point of the perturbation. This means that we vary the unperturbed Hamiltonian  $H_0$  in order to improve the results. Of course, the total Hamiltonian  $H = H_0 + H_P$  may not be changed so that a variation of  $H_0$  will automatically imply a variation of the perturbing part  $H_P$ .

Let us assume that  $H_0$  depends on some parameter  $u$  or on a set of parameters  $\vec{u}$  which we may vary. How does one determine the appropriate starting point  $H_0(u_0)$  for the perturbation? In this issue we follow the principle of minimal sensitivity<sup>19</sup>. The underlying idea is that the exact diagonalization of  $H$  does not depend on the starting point  $u_0$ . This, of course, will not be true for a generic approximative scheme. Thus a quantity such as the ground state energy  $E_0$  will depend on  $u$  if computed approximately:  $E_0^{\text{app}}(u)$ . Then, the principle of minimal sensitivity suggests to choose  $u_0$  such that  $E_0^{\text{app}}(u)$  depends minimally on  $u$  in the vicinity of  $u_0$ . Thus, one should choose local extrema or saddle points to determine the starting value  $u_0$ . Given that  $E_0^{\text{app}}(u)$  is differentiable one obtains as defining equation

$$\left. \partial_u E_0^{\text{app}}(u) \right|_{u=u_0} = 0. \quad (2)$$

Note that for  $n$  parameters  $u_i$  the above prescription implies  $n$  equations  $\partial_{u_i} E_0^{\text{app}}(\vec{u})|_{\vec{u}=\vec{u}_0} = 0$  to determine  $\vec{u}_0$ . In case that  $E_0^{\text{app}}(\vec{u})$  is not differentiable at the points of interest we look for local extrema or saddle points. This is analogous to standard thermodynamics where the physical phase is represented by a local extrema or saddle points of a thermodynamic potentials. Cusps may occur as well and they generically indicate first order transitions. This exemplifies that the non-differentiability does not invalidate the prescription to look for local extrema or saddle points.

If the perturbation is performed around a bilinear bosonic Hamiltonian the dependence  $H_0(u)$  may equivalently be replaced by the dependence of the set  $\{a_i(u)\}$  of annihilation operators and the corresponding creation operators which diagonalize  $H_0(u)$ . This approach has been used to illustrate the usefulness of the principle of minimal sensitivity in perturbative calculations and for continuous unitary transformations<sup>19,20</sup>. Below, we will use it to improve perturbative spin wave calculations for the Heisenberg model on a square lattice. The spin operators will be represented as introduced by Dyson and Maleev<sup>21-24</sup> so that the bosonic approach can be directly put to use.

The article is set up as follows. In the following section II, we introduce the model and its bosonic representation.

In particular, the variation of the bosonic description will be explained. In Sect. III we present results for the variation in two parameters. Results for the ground state energy and for the dispersion are shown. Finally, the article is concluded in Sect. IV.

## II. MODEL AND METHOD

### A. Model

Expressed in the usual spin operators the Hamiltonian is given in Eq. (1). Exploiting that the square lattice is bipartite we may write

$$H = J \sum_{i \in \Gamma_A, \delta} \mathbf{S}_i^A \cdot \mathbf{S}_{i+\delta}^B, \quad (3)$$

where  $\Gamma_A$  is the lattice made only from all  $A$  sites. Finally, we will focus on  $S = 1/2$ . But for introducing the bosonic representation it is convenient to treat general spin. We use the Dyson-Maleev representation<sup>21-24</sup>

$$S_{Ai}^+ = \sqrt{2S} \left[ a_i - \frac{a_i^\dagger a_i a_i}{(2S)} \right], \quad S_{Ai}^- = \sqrt{2S} a_i^\dagger, \quad (4a)$$

$$S_{Ai}^z = S - a_i^\dagger a_i, \quad (4a)$$

$$S_{Bj}^+ = \sqrt{2S} \left[ b_j^\dagger - \frac{b_j^\dagger b_j^\dagger b_j}{(2S)} \right], \quad S_{Bj}^- = \sqrt{2S} b_j, \quad (4b)$$

$$S_{Bj}^z = -S + b_j^\dagger b_j, \quad (4b)$$

where  $a_i^{(\dagger)}$  are bosonic creation/annihilation operators on the  $A$ -sites and  $b_i^{(\dagger)}$  on the  $B$ -sites. Next, we transform these bosonic operators in momentum space. We stress that the momenta  $\mathbf{k}$  are taken from the magnetic Brillouin zone (MBZ), which is a tilted square in  $k$ -space with the corners  $(\pm\pi, 0)$  and  $(0, \pm\pi)$ , because the real space coordinate  $i$  runs over  $\Gamma_A$ .

### B. Basic Steps

Next, we perform a conventional Bogoliubov transformation respecting translational invariance

$$\alpha_{\mathbf{k}}^\dagger = l_{\mathbf{k}} \alpha_{\mathbf{k}}^\dagger + m_{\mathbf{k}} \beta_{-\mathbf{k}}, \quad b_{-\mathbf{k}} = m_{\mathbf{k}} \alpha_{\mathbf{k}}^\dagger + l_{\mathbf{k}} \beta_{-\mathbf{k}}, \quad (5)$$

where  $\alpha_{\mathbf{k}}^{(\dagger)}$  and  $\beta_{\mathbf{k}}^{(\dagger)}$  are the new operators in which we express the Hamiltonian. The prefactors  $l_{\mathbf{k}}$  and  $m_{\mathbf{k}}$  can be chosen at will as long as they fulfil  $l_{\mathbf{k}}^2 + m_{\mathbf{k}}^2 = 1$  where we assume them to be real. The freedom of choice for these prefactors provides us with the possibility to choose the starting point of the perturbation theory as described in the Introduction. Below, in Sect. IID, we will specify how  $l_{\mathbf{k}}$  and  $m_{\mathbf{k}}$  depend on the variational parameters.

We find it convenient to parametrize the prefactors by

$$l_{\mathbf{k}} = \left[ \frac{1 + \mu_{\mathbf{k}}}{2\mu_{\mathbf{k}}} \right]^{1/2}, \quad m_{\mathbf{k}} = - \left[ \frac{1 - \mu_{\mathbf{k}}}{2\mu_{\mathbf{k}}} \right]^{1/2} =: -x_{\mathbf{k}} l_{\mathbf{k}},$$

$$x_{\mathbf{k}} = \left[ \frac{1 - \mu_{\mathbf{k}}}{1 + \mu_{\mathbf{k}}} \right]^{1/2}, \quad (6)$$

where  $\mu_{\mathbf{k}}$  can still be chosen freely as long as  $|\mu_{\mathbf{k}}| \leq 1$  holds. To elucidate the above parametrization we recall that the choice

$$\mu_{\mathbf{k}} = \sqrt{1 - \gamma_{\mathbf{k}}^2} \quad \gamma_{\mathbf{k}} := \frac{1}{2}(\cos(k_x) + \cos(k_y)) \quad (7)$$

leads to the standard linear spin wave description. We will come back to this point in Sect. IID where we will specify how  $\mu_{\mathbf{k}}$  is modified as function of variational parameters.

First, however, we express the Hamiltonian in the fields  $\alpha_{\mathbf{k}}^{(\dagger)}$  and  $\beta_{\mathbf{k}}^{(\dagger)}$ . We split it according to

$$H = H_{\text{cl}} + H_{\text{bl}} + H_{\text{ql}}, \quad (8)$$

where  $H_{\text{cl}} = -4JS^2N$  simply stands for the classical ground state energy; note that here  $N$  is the number of  $A$ -sites. The second term  $H_{\text{bl}}$  stands for the part which stems from the bilinear terms if  $H$  is expressed in the original bosonic fields in (4). It reads

$$H_{\text{bl}} = E_{01} + H_{\text{D1}} + H_{\text{B1}}, \quad (9)$$

where

$$E_{01} := 8JS \sum_{\mathbf{k} \in \text{MBZ}} l_{\mathbf{k}}^2 x_{\mathbf{k}} (x_{\mathbf{k}} - \gamma_{\mathbf{k}}) \quad (10a)$$

$$H_{\text{D1}} := 4JS \sum_{\mathbf{k} \in \text{MBZ}} A_{1\mathbf{k}} (\alpha_{\mathbf{k}}^{\dagger} \alpha_{\mathbf{k}} + \beta_{\mathbf{k}}^{\dagger} \beta_{\mathbf{k}}) \quad (10b)$$

$$H_{\text{B1}} := 4JS \sum_{\mathbf{k} \in \text{MBZ}} B_{1\mathbf{k}} (\alpha_{\mathbf{k}}^{\dagger} \beta_{-\mathbf{k}}^{\dagger} + \text{h.c.}). \quad (10c)$$

The momentum dependent prefactors are given by

$$A_{1\mathbf{k}} := l_{\mathbf{k}}^2 (1 - 2x_{\mathbf{k}} \gamma_{\mathbf{k}} + x_{\mathbf{k}}^2) \quad (11a)$$

$$B_{1\mathbf{k}} := l_{\mathbf{k}}^2 (\gamma_{\mathbf{k}} - 2x_{\mathbf{k}} + \gamma_{\mathbf{k}} x_{\mathbf{k}}^2). \quad (11b)$$

Doing the same for the quartic part  $H_{\text{ql}}$  yields

$$H_{\text{ql}} = E_{02} + H_{\text{D2}} + H_{\text{B2}} + H_{\text{V}}, \quad (12)$$

with

$$E_{02} := -JNA_2^2 \quad (13a)$$

$$A_2 := \frac{2}{N} \sum_{\mathbf{k} \in \text{MBZ}} l_{\mathbf{k}}^2 (x_{\mathbf{k}} \gamma_{\mathbf{k}} - x_{\mathbf{k}}^2) \quad (13b)$$

$$H_{\text{D2}} := 2J \sum_{\mathbf{k} \in \text{MBZ}} A_{2\mathbf{k}} (\alpha_{\mathbf{k}}^{\dagger} \alpha_{\mathbf{k}} + \beta_{\mathbf{k}}^{\dagger} \beta_{\mathbf{k}}) \quad (13c)$$

$$H_{\text{B2}} := 2J \sum_{\mathbf{k} \in \text{MBZ}} B_{2\mathbf{k}} (\alpha_{\mathbf{k}}^{\dagger} \beta_{-\mathbf{k}}^{\dagger} + \text{h.c.}), \quad (13d)$$

where we find

$$A_{2\mathbf{k}} = A_2 \cdot A_{1\mathbf{k}} \quad (14a)$$

$$B_{2\mathbf{k}} = A_2 \cdot B_{1\mathbf{k}}. \quad (14b)$$

Of course, the simplicity of the last relation results from the simplicity of the original model which is characterized only by nearest neighbor couplings which are all renormalized by the mean-field effects in the same way.

The quadrilinear interaction part is given by the normal-ordered expression

$$H_{\text{V}} = -\frac{J}{N} \sum_{1234} \delta_{12}^{34} l_1 l_2 l_3 l_4 \left[ V_{1234}^{(1)} \alpha_1^{\dagger} \alpha_2^{\dagger} \alpha_3 \alpha_4 \right. \\ + 2V_{1234}^{(2)} \alpha_1^{\dagger} \beta_{-2} \alpha_3 \alpha_4 + 2V_{1234}^{(3)} \alpha_1^{\dagger} \alpha_2^{\dagger} \beta_{-3}^{\dagger} \alpha_4 \\ + 4V_{1234}^{(4)} \alpha_1^{\dagger} \alpha_3 \beta_{-4}^{\dagger} \beta_{-2} + 2V_{1234}^{(5)} \beta_{-4}^{\dagger} \alpha_3 \beta_{-2} \beta_{-1} \\ + 2V_{1234}^{(6)} \beta_{-4}^{\dagger} \beta_{-3}^{\dagger} \alpha_2^{\dagger} \beta_{-1} + V_{1234}^{(7)} \alpha_1^{\dagger} \alpha_2^{\dagger} \beta_{-3}^{\dagger} \beta_{-4}^{\dagger} \\ \left. + V_{1234}^{(8)} \beta_{-1} \beta_{-2} \alpha_3 \alpha_4 + V_{1234}^{(9)} \beta_{-4}^{\dagger} \beta_{-3}^{\dagger} \beta_{-2} \beta_{-1} \right], \quad (15)$$

where the subscripts  $i = 1, 2, 3, 4$  stand for the momenta  $\mathbf{k}_i$  and  $-i$  stands for  $-\mathbf{k}_i$ . The conservation of momentum in the lattice is ensured by the Kronecker symbol  $\delta_{12}^{34}$  which implies  $\mathbf{k}_1 + \mathbf{k}_2 = \mathbf{k}_3 + \mathbf{k}_4$  modulo reciprocal lattice vectors from the reciprocal lattice  $\Gamma_A^*$  of the  $A$ -sites, i.e.,  $\mathbf{g} \in \Gamma_A^*$  means  $\mathbf{g} = (n\pi, m\pi)$  with the integers  $n, m$  if the lattice constant of the original square lattice is set to unity. The vertex functions  $V_{1234}^{(i)}$  are given explicitly in App. A.

Now we can combine the diagonal parts in

$$H_{\text{D}} := E_{00} + H_{\text{D1}} + H_{\text{D2}} \quad (16a)$$

$$= E_{00} + 4J \sum_{\mathbf{k} \in \text{MBZ}} \omega_{\mathbf{k}} (\alpha_{\mathbf{k}}^{\dagger} \alpha_{\mathbf{k}} + \beta_{\mathbf{k}}^{\dagger} \beta_{\mathbf{k}}) \quad (16b)$$

$$E_{00} := H_{\text{cl}} + E_{01} + E_{02} \quad (16c)$$

$$= -4JS^2N - J(4SA_2 + A_2^2)N \quad (16d)$$

$$\omega_{\mathbf{k}} = (S + \frac{1}{2}A_2)l_{\mathbf{k}}^2(1 - 2x_{\mathbf{k}}\gamma_{\mathbf{k}} + x_{\mathbf{k}}^2) \quad (16e)$$

and the perturbing part  $H_{\text{P}}$  in

$$H_{\text{P}} := H_{\text{B}} + H_{\text{V}} \quad (17a)$$

$$H_{\text{B}} := 4J \sum_{\mathbf{k} \in \text{MBZ}} B_{\mathbf{k}} (\alpha_{\mathbf{k}}^{\dagger} \beta_{-\mathbf{k}}^{\dagger} + \text{h.c.}) \quad (17b)$$

$$B_{\mathbf{k}} := (S + \frac{1}{2}A_2)l_{\mathbf{k}}^2(\gamma_{\mathbf{k}} - 2x_{\mathbf{k}} + \gamma_{\mathbf{k}} x_{\mathbf{k}}^2) \quad (17c)$$

where  $H_{\text{B}}$  in (17a) stems from the sum  $H_{\text{B1}} + H_{\text{B2}}$ .

### C. Approximate Evaluation

A straightforward procedure is to use standard perturbation theory in  $H_{\text{V}}$ , for instance in second order, to compute the ground state energy  $E_0$  and the dispersion  $\omega(\mathbf{k})$  in an approximate way. (Note the difference between  $\omega_{\mathbf{k}}$ ,

the dispersion in the unperturbed Hamiltonian  $H_D$  and the dispersion  $\omega(\mathbf{k})$  of the full Hamiltonian.) First, we focus on the ground state energy because its local saddle point (2) will determine  $\{\mu_{\mathbf{k}}\}$ . The correction  $\Delta E_B$  due to  $H_B$  can be easily computed to infinite order in  $B_{\mathbf{k}}$  analytically by Bogoliubov transformation

$$\Delta E_B = -2JN(2S + A_2)(\mathcal{A}_2 - A_2), \quad (18)$$

where  $\mathcal{A}_2$  is the value for  $A_2$  if we diagonalize the bilinear Hamiltonian from the very beginning, i.e.,  $\mathcal{A}_2 = A_2$  as given by Eq. (13b) for  $\mu_{\mathbf{k}} = \sqrt{1 - \gamma_{\mathbf{k}}^2}$ . The correction  $\Delta E_V$  involving  $H_V$  are much more complicated so that we determine them only in second order in  $H_V$

$$\Delta E_V = -\frac{J}{N^2} \sum_{1234} \frac{\delta_{12}^{34} (l_1 l_2 l_3 l_4)^2 V_{1234}^{(7)} V_{4321}^{(8)}}{\omega_1 + \omega_2 + \omega_3 + \omega_4} \quad (19)$$

Formally, there could also be a second order contribution which is linear in  $H_B$  and in  $H_V$ , but no such term contributes to the ground state energy. Hence the approximate ground state energy  $E_0$  is given by

$$E_0 = E_{00} + \Delta E_B + \Delta E_V. \quad (20)$$

In the same fashion, we compute the dispersion. The influence of  $H_B$  is again taken into account in infinite order yielding

$$\omega_B(\mathbf{k}) = 2J(2S + A_2)\sqrt{1 - \gamma_{\mathbf{k}}^2}. \quad (21)$$

The additional second order correction  $\Sigma_V(\mathbf{k})$  reads

$$\Sigma_V(\mathbf{k}) = \Sigma_{BV}(\mathbf{k}) + \Sigma_{VV}(\mathbf{k}) \quad (22a)$$

$$\Sigma_{BV}(\mathbf{k}) = \frac{2Jl_{\mathbf{k}}^2}{N} \sum_{\mathbf{p}} \frac{l_{\mathbf{p}}^2}{\omega_{\mathbf{p}}} B_{\mathbf{p}}(V_{\mathbf{kppk}}^{(2)} + V_{\mathbf{kppk}}^{(3)}) \quad (22b)$$

$$\Sigma_{VV}(\mathbf{k}) = \frac{2Jl_{\mathbf{k}}^2}{N^2} \sum_{\mathbf{p}, \mathbf{q}, \mathbf{s}} (l_{\mathbf{p}} l_{\mathbf{q}} l_{\mathbf{s}})^2 \delta_{\mathbf{kp}}^{\mathbf{qs}} \left[ \frac{V_{\mathbf{kpqs}}^{(2)} V_{\mathbf{sqpk}}^{(3)}}{\omega_{\mathbf{k}} - \omega_{\mathbf{p}} - \omega_{\mathbf{q}} - \omega_{\mathbf{s}}} - \frac{V_{\mathbf{kpqs}}^{(7)} V_{\mathbf{sqpk}}^{(8)}}{\omega_{\mathbf{k}} + \omega_{\mathbf{p}} + \omega_{\mathbf{q}} + \omega_{\mathbf{s}}} \right] \quad (22c)$$

so that the total approximate dispersion finally is given by

$$\omega(\mathbf{k}) = \omega_B(\mathbf{k}) + \Sigma_V(\mathbf{k}). \quad (23)$$

Note that in the quadratic correction  $\Sigma_{BV}(\mathbf{k})$  both perturbing terms  $H_B$  and  $H_V$  enter.

#### D. Variation of $H_D$

The equations similar to the above can be found in many previous approaches<sup>2,7-10</sup>. The main difference is that in the previous equations  $\mu_{\mathbf{k}}$  was chosen such that  $H_B$  vanished or appeared only in subdominant orders

in  $1/S$ . The equations above for arbitrary  $\mu_{\mathbf{k}}$  are more general. They allow us to vary what we call an  $\alpha_{\mathbf{k}}^\dagger$  or  $\beta_{\mathbf{k}}^\dagger$  excitation. Thereby, the diagonal part of the perturbation  $H_D$  is varied and we can apply the principle of minimal sensitivity by looking for local saddle points of  $E_0$  as it results from the approximate calculation.

Pursuing this line of argument we should vary  $\mu_{\mathbf{k}}$  at each point in the magnetic Brillouin zone in the range  $1 \geq |\mu_{\mathbf{k}}|$ . This, however, is far too ambitious because of the macroscopic number of parameters to be varied. Thus, to simplify the approach we choose a particular parametrization of  $\mu_{\mathbf{k}}$  which relies only on a small number of parameters. In the present work, we want to illustrate the approach in principle and restrict ourselves to two free parameters. Moreover, it is reasonable to choose  $\mu_{\mathbf{k}}$  close to  $\sqrt{1 - \gamma_{\mathbf{k}}^2}$  which would correspond to the correct solution in the limit  $S \rightarrow \infty$ . Therefore, our choice is

$$\mu_{\mathbf{k}} = (1 - f_{\mathbf{k}})\sqrt{1 - \gamma_{\mathbf{k}}^2}, \quad (24)$$

where

$$f_{\mathbf{k}} := v \cos(k_x) \cos(k_y) + |v| + u(\cos(k_x) + \cos(k_y) - 2) \quad (25a)$$

for  $u \leq |v|/4$  and

$$f_{\mathbf{k}} := v \cos(k_x) \cos(k_y) + u(\cos(k_x) + \cos(k_y) + 2) \quad (25b)$$

otherwise. The above choice is motivated by two arguments. First, we intend to include the cosine terms which go beyond nearest neighbor processes. The simplest choice are the two next-nearest neighbor processes included above. Second,  $f_{\mathbf{k}}$  may not become negative because  $|\mu_{\mathbf{k}}|$  can exceed unity in this case. This is particularly important at the border of the magnetic Brillouin zone where  $\gamma_{\mathbf{k}} = 0$ . In addition,  $f_{\mathbf{k}}$  may not exceed unity because  $\mu_{\mathbf{k}}$  should not change sign. This implies that  $u$  and  $v$  may not be chosen too large.

On the boundary, i.e., for  $\gamma_{\mathbf{k}} = 0$ , we choose  $k_x = q$ ,  $k_y = \pi - q$  and obtain for  $u \leq |v|/4$

$$f_q = (v/2 - 2u)(1 - \cos(2q)) + |v| - v \quad (26a)$$

and  $u \geq |v|/4$

$$f_q = (2u - v/2)(1 + \cos(2q)). \quad (26b)$$

We see that  $f_q \geq 0$  is ensured. Note for future reference that for  $u = v/4$  no dispersion along the boundary of the magnetic Brillouin zone occurs so that this line is special.

### III. RESULTS

The results presented below are evaluated for  $S = 1/2$ . First, we analyze the dependence of the ground state energy on the chosen parameters. It turns out that the most interesting parameter region is  $u, v \geq 0$ .

### A. Ground State Energy

Fig. 1 shows the energy dependence of  $E_0$  as given by (20) on the two parameters  $u$  and  $v$ . Obviously, no dominant local minima or maxima catch our eye in the upper panel. In the lower panel, one can presume a saddle point in the center of the figure. Generally, very little dependence on  $u$  and  $v$  occurs in the middle region displayed in the lower panel.

Closer inspection of this range of  $u$  and  $v$ , see Fig. 2, shows that there is a line of small cusps given by  $u = v/4$  as long as  $v$  is not too large, see also right panel of Fig. 3 below. In view of the definition of  $f_{\mathbf{k}}$  in (25) the appearance of such a cusp may not surprise. In addition, the line  $u = v/4$  is special since it makes any dispersion at the magnetic Brillouin zone boundary vanish.

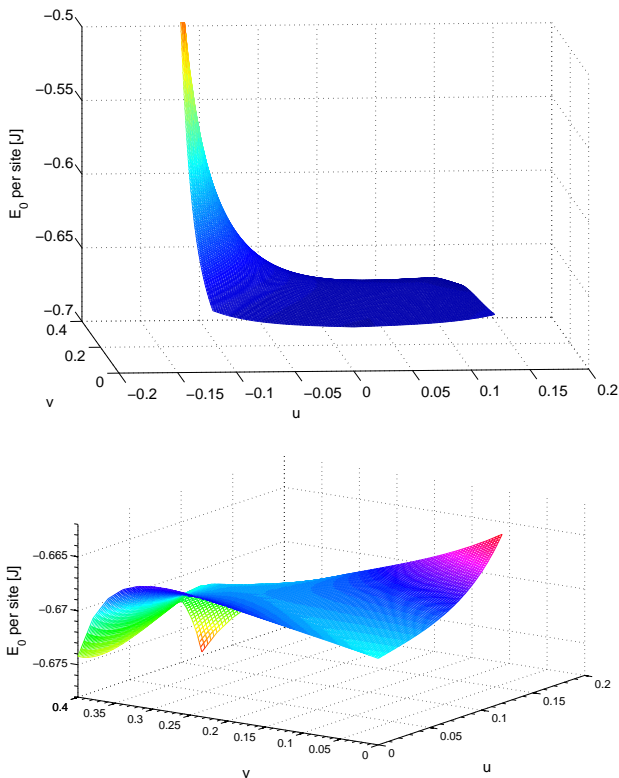


FIG. 1: (Color online) Approximate ground state energy  $E_0(u, v)$  per site of the original lattice, i.e.,  $E_0/(2N)$ , as computed by Eq. (20). If the calculation were exact,  $E_0$  should be constant. Due to the approximations used this is not the case. The best strategy is to look for local extrema or saddle points because they represent points where  $E_0$  is stationary at least locally. Upper panel: Overall view, no extrema or saddle points are discernible. Lower panel: For  $u \geq 0$ , the energy landscape displays more structure and a saddle point can be presumed in the middle of the figure. Note that for clarity the color coding in the lower panel is different from the one in the upper panel.

To elucidate the energy behavior more quantitatively

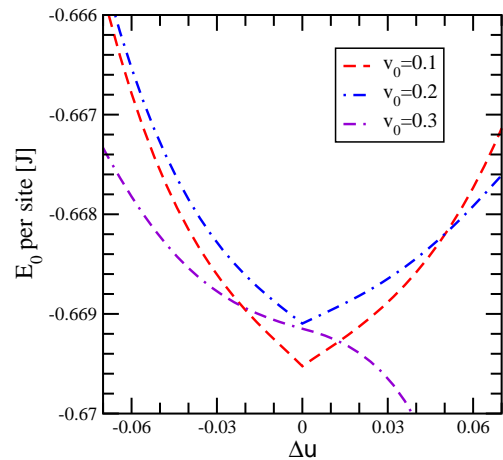


FIG. 2: (Color online) Cuts of  $E_0(u, v)/(2N)$  perpendicular to the line  $u = v/4$  along the line  $(u_0 + \Delta u, v_0 - \Delta u/4)$ . The cusps at  $\Delta u = 0$  for not too large  $v_0$  are obvious.

Fig. 3 shows two perpendicular cuts through the energy landscape of Fig. 1. The left panel in Fig. 3 follows the line of cusps along  $u = v/4$ . Clearly, a local maximum appears which is located at  $v_0 = 0.2502(1)$ . But the dependence through this point along a line perpendicular to  $u = v/4$  displays the cusp at  $v_0$  which is a local minimum. Note, that the definition (25) is prone to yield cusps as stated above. But it is a priori not clear that these cusps are extrema in certain directions. Since the point at  $(v_0/4, v_0)$  is a local minimum in one direction, but a local maximum in the perpendicular direction we are not observing a local extremum, but a saddle point though  $E_0(u, v)$  is not differentiable in one direction. If  $E_0$  were differentiable, for instance if it were smeared out a tiny bit by convolution with a narrow Gaussian, it would display a usual saddle point very close to  $(v_0/4, v_0)$ . We interpret the occurrence of this special point on the line  $(v/4, v)$  as evidence that the optimum  $\mu_{\mathbf{k}}$  should not display a finite dispersion on the boundary of the magnetic Brillouin zone, cf. Eq. (26).

For the precise determination of  $v_0$ , calculations are done for various system sizes with linear extensions  $L = 24, 32, 36$ . The extrapolation of the position of the local maximum yields  $v_0 = 0.2502(1)$  and the energy value at this position is found to be  $E_0/(2N) = -0.66902(2)J$ . These values should be compared to the quantum Monte Carlo result<sup>25</sup>  $E_0/(2N) = -0.669437(5)J$  and to the second order result of a plain  $1/S$  expansion<sup>8</sup> which reads  $E_0/(2N) = -0.66999J$ . (Note that this number is referred to as “third order” in Ref. 8 because the authors include the classical energy in their power counting.) If we take the Monte Carlo expansion as reliable reference the variation of second order perturbation theory could reduce the deviation from  $0.0006J$  to  $-0.0004J$  which is a reduction by about 25%. To judge the improvement we point out that passing from rather simple first order perturbative spin wave theory  $E_0/(2N) = -0.67042J$  to second order  $E_0/(2N) = -0.66999J$  improved the ground

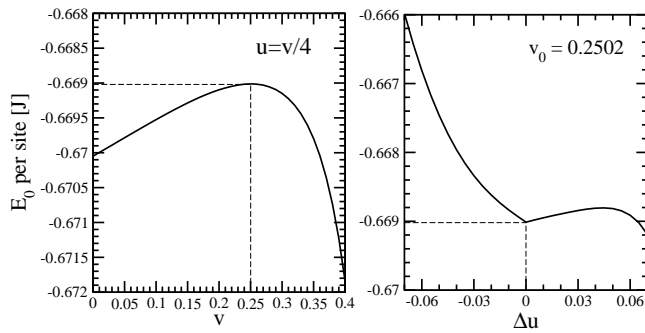


FIG. 3: Cuts of  $E_0(u, v)/(2N)$  along special lines. Left panel: along the lines of cusps  $u = v/4$ . Clearly a local maximum appears at  $v_0 = 0.2502$ . Right panel: This cut follows the line through the point  $(u_0 = v_0/4, v_0)$ , but perpendicular to  $u = v/4$ . It is given by  $(u_0 + \Delta u, v_0 - \Delta u/4)$ . The cusp at  $\Delta u = 0$  is obvious.

state energy by 44%.

We also stress that the improved result  $E_0/(2N) = -0.66902(2)J$  is obtained by using equations of the same complexity as the second order equations. The add-on is just the variation of the unperturbed starting point. In higher orders, this variation becomes an even more efficient tool, see Ref. 20 for the discussion of the example of the quartic oscillator.

In the end, however, our goal is not to obtain estimates for the ground state energy in the first place. In the varied perturbation theory, the analysis of the ground state energy primarily serves the purpose to fix the unperturbed starting point  $H_D$ .

## B. Magnon Dispersion

Above, we have determined the optimum starting point  $H_D(u, v)$  by analysing the dependence of the approximate ground state energy. We identified the optimum starting point to be given by  $(v_0/4, v_0)$  with  $v_0 = 0.2502(1)$  where a saddle point appeared. Next, we use this starting point to analyze the magnon dispersion in general and the dip between the values at  $(\pi, 0)$  and at  $(\pi/2, \pi/2)$  in particular.

Fig. 4 depicts the corresponding result compared with results from first and second order perturbative spin wave theory. First, we find that the overall shape of all three curves is very similar. This was expected from the comparison of various perturbative results, high order series expansion and quantum Monte Carlo data, see Fig. 1 in Ref. 10.

Second, the dip at  $(\pi, 0)$  relative to the dispersion at  $(\pi/2, \pi/2)$  is more pronounced in the varied perturbation theory. We find that the dip takes the relative value 3.3(1)% which is rather precisely the value which Syromyatnikov found in the much more complex third order perturbation calculation<sup>10</sup>. It improves the second order result of 1.4% by more than a factor of 2 while it

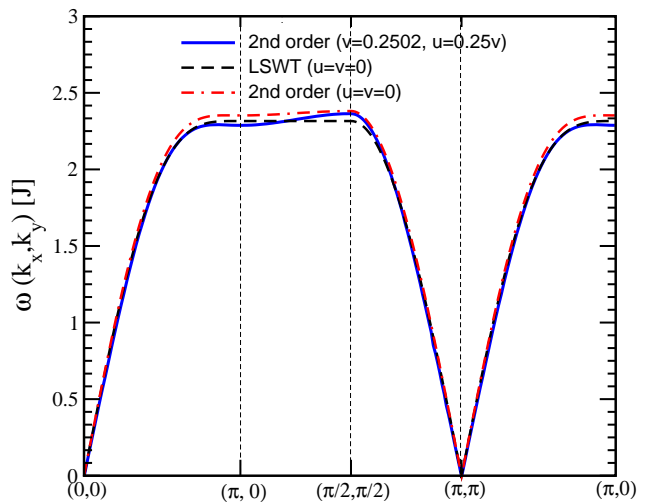


FIG. 4: (Color online) Dispersion of the Heisenberg lattice model in (i) linear spin wave theory (LSWT) including first order corrections, (ii) second order perturbation theory around the LSWT solution, i.e., for  $(u, v) = (0, 0)$ , (iii) in varied second order perturbation theory around  $(v_0/4, v_0)$  with  $v_0 = 0.2502$  which corresponds to the saddle point of the ground state energy.

is still away from the about 9% of dip obtained by series expansion<sup>5</sup> or quantum Monte Carlo<sup>6</sup>.

In detail, we find  $\omega(\pi, 0) = 2.2881(1)J$  and  $\omega(\pi/2, \pi/2) = 2.3643(2)J$ . The latter value is very close to the series value  $\omega^{\text{series}}(\pi/2, \pi/2) = 2.385(1)J$  and to the quantum Monte Carlo value  $\omega^{\text{QMC}}(\pi/2, \pi/2) = 2.39J$ . The former is still by about 5% too high compared to  $\omega^{\text{series}}(\pi, 0) = 2.18(1)J$  and  $\omega^{\text{QMC}}(\pi, 0) = 2.16J$ . So there is still some way to go.

But to judge the numbers obtained by varied perturbation theory we also compare to the ordinary second order perturbative numbers  $\omega^{2\text{nd}}(\pi, 0) = 2.3586J$  and  $\omega^{2\text{nd}}(\pi/2, \pi/2) = 2.3920J$  and to the third order perturbative numbers  $\omega^{3\text{rd}}(\pi, 0) = 2.3241(2)J$  and  $\omega^{3\text{rd}}(\pi/2, \pi/2) = 2.4007(2)J$ . Relative to these numbers, the varied perturbative results represent an improvement, in particular in comparison to the plain second order results. It must be kept in mind that the varied perturbation theory is based essentially on the same equations as the plain second order results. Thus one achieves third order accuracy, see results by Syromyatnikov in Ref. 10, for the effort of the second order calculation.

These findings show that the variation of perturbative calculations indeed reduces deviations to the exact results. In this way, improved results are accessible without resorting to more complex higher order calculations.

## IV. CONCLUSIONS

In summary, we investigated the Heisenberg quantum antiferromagnet in terms of spin waves (magnons) based on the Dyson-Maleev representation. The primary goal was to determine the dispersion of the magnons. A secondary goal was the determination of the ground state energy.

The approach employed for evaluation is based on standard perturbation theory. But we do not pursue a plain expansion in  $1/S$ . Instead, we choose the unperturbed Hamiltonian  $H_D$ , which serves as starting point, arbitrarily among bilinear bosonic operators. In the present article, we did not exploit the full freedom of choice of such operators but investigated a parametrization with two variables  $(u, v)$  which remains close to the bilinear bosonic Hamiltonian of linear spin wave theory. Considering more variables would have obscured the fundamental principle of the approach and it would have been rather cumbersome on the technical level.

Following the principle of minimal sensitivity, we search the parameter space  $(u, v)$  for stationary points, i.e., local extrema or saddle points, of  $E_0(u, v)$ . Thus the approach is called varied perturbation theory. Such a point is indeed found at  $(u_0 = v_0/4, v_0)$  with  $v_0 = 0.2502(1)$ . Due to non-differentiability, it is not an ordinary saddle point, but a point with a cusp-like minimum in one direction and a differentiable maximum in the perpendicular direction.

At this saddle point, the value of the ground state energy is closer to the exact value than the plain second order perturbation. Furthermore, the magnon dispersion obtained at this saddle point displays a more significant dip of 3.3% which is again more than twice as large as the plain second order calculation provides. The plain third order calculation yields a comparable dip of 3.2% which means that the variation of the starting point allowed us to obtain third order accuracy with the effort of a second order calculation. This represents the methodological achievement. The agreement with high order series results and quantum Monte Carlo data is still unsatisfactory because these approaches find a dip of about 9%.

We attribute the remaining discrepancy to the low order (here: second order) perturbative approach which we employed to calculate  $E_0(u, v)$ . We expect that a varied third order approach enhances the dip to about 6 – 7% percent, combining the factors of 2 from the variation

(this article) and from passing from second to third order (Ref. 10).

Previous investigations of the simple model of a quartic oscillator have shown that the variation of the starting point combined with improved evaluation schemes such as higher order perturbation theory<sup>19</sup> or continuous unitary transformation<sup>20</sup> is capable to provide very good quantitative results.

The progress achieved in this article is two-fold: On the methodological side, we introduced the principle of minimal sensitivity in the calculation for an exemplary extended solid state system displaying important correlations.

On the physical side, we provided evidence that the dip in the dispersion of the square lattice Heisenberg antiferromagnet with  $S = 1/2$  can be explained in terms of magnons if more advanced approaches are used. In our opinion, one does not have to resort to fractionalization into spinons as sometimes discussed<sup>13</sup> in order to understand the dip.

But we admit that a quantitative reproduction of the dip has not yet been achieved so that further work is called for. Promising improved approaches to reach this goal comprise third order perturbative approaches and continuous unitary transformations<sup>26</sup>.

## Acknowledgments

We acknowledge the Texas Advanced Computing Center (TACC) at The University of Texas at Austin for providing HPC resources that have contributed to part of the research results reported within this paper. Part of this work was also done at the HPC cluster at GVSU which is supported by the National Science Foundation Grant No. CNS-1228291. We acknowledge financial support by the NRW Forschungsschule “Forschung mit Synchrotronstrahlung in den Nano- und Biowissenschaften” and by the the Helmholtz Virtual Institute “New states of matter and their excitations”.

## Appendix A: Vertex Functions

Below, we use  $x_i$  for  $x_{\mathbf{k}_i}$  and  $\gamma(i)$  for  $\gamma(\mathbf{k}_i)$ ,  $\gamma(i-j)$  for  $\gamma(\mathbf{k}_i - \mathbf{k}_j)$ , and so on. The vertex functions are given by

$$V_{1234}^{(1)} = x_1x_3\gamma(1-3) + x_1x_4\gamma(1-4) + x_2x_3\gamma(2-3) + x_2x_4\gamma(2-4) - x_1\gamma(1) - x_2\gamma(2) - x_1x_3x_4\gamma(1-3-4) - x_2x_3x_4\gamma(2-3-4), \quad (\text{A1a})$$

$$V_{1234}^{(2)} = -x_3\gamma(2-3) - x_4\gamma(2-4) - x_1x_2x_3\gamma(1-3) - x_1x_2x_4\gamma(1-4) + x_1x_2\gamma(1) + \gamma(2) + x_1x_2x_3x_4\gamma(1-3-4) + x_3x_4\gamma(2-3-4), \quad (\text{A1b})$$

$$V_{1234}^{(3)} = -x_1\gamma(1-3) - x_2\gamma(2-3) - x_1x_3x_4\gamma(1-4) - x_2x_3x_4\gamma(2-4) + x_1x_3\gamma(1) + x_2x_3\gamma(2) + x_1x_4\gamma(1-3-4) + x_2x_4\gamma(2-3-4), \quad (\text{A1c})$$

$$V_{1234}^{(4)} = x_1x_2x_3x_4\gamma(1-3) + x_1x_2\gamma(1-4) + x_3x_4\gamma(2-3) + \gamma(2-4) - x_4\gamma(2) - x_1x_2x_4\gamma(1) - x_3\gamma(2-3-4) - x_1x_2x_3\gamma(1-3-4), \quad (\text{A1d})$$

$$V_{1234}^{(5)} = -x_2x_3x_4\gamma(1-3) - x_1x_3x_4\gamma(2-3) - x_1\gamma(2-4) - x_2\gamma(1-4) + x_1x_4\gamma(2) + x_2x_4\gamma(1) + x_1x_3\gamma(2-3-4) + x_2x_3\gamma(1-3-4), \quad (\text{A1e})$$

$$V_{1234}^{(6)} = -x_4\gamma(1-3) - x_3\gamma(1-4) - x_1x_2x_3\gamma(2-4) - x_1x_2x_4\gamma(2-3) + \gamma(1-3-4) + x_1x_2\gamma(2-3-4) + x_3x_4\gamma(1) + x_1x_2x_3x_4\gamma(2), \quad (\text{A1f})$$

$$V_{1234}^{(7)} = x_1x_4\gamma(1-3) + x_1x_3\gamma(1-4) + x_2x_3\gamma(2-4) + x_2x_4\gamma(2-3) - x_1x_3x_4\gamma(1) - x_2x_3x_4\gamma(2) - x_1\gamma(1-3-4) - x_2\gamma(2-3-4), \quad (\text{A1g})$$

$$V_{1234}^{(8)} = x_1x_4\gamma(2-4) + x_2x_4\gamma(1-4) + x_1x_3\gamma(2-3) + x_2x_3\gamma(1-3) - x_1\gamma(2) - x_2\gamma(1) - x_1x_3x_4\gamma(2-3-4) - x_2x_3x_4\gamma(1-3-4), \quad (\text{A1h})$$

$$V_{1234}^{(9)} = x_1x_3\gamma(2-4) + x_2x_3\gamma(1-4) + x_1x_4\gamma(2-3) + x_2x_4\gamma(1-3) - x_1\gamma(2-3-4) - x_2\gamma(1-3-4) - x_1x_3x_4\gamma(2) - x_2x_3x_4\gamma(1). \quad (\text{A1i})$$

\* Electronic address: [goetz.uhrig@tu-dortmund.de](mailto:goetz.uhrig@tu-dortmund.de)

† Electronic address: [majumdar@gvsu.edu](mailto:majumdar@gvsu.edu)

- <sup>1</sup> E. Manousakis, *Rev. Mod. Phys.* **63**, 1 (1991).
- <sup>2</sup> K. Majumdar, D. Furton, and G. S. Uhrig, *Phys. Rev. B* **85**, 144420 (2012).
- <sup>3</sup> M. Le Tacon, G. Ghiringhelli, J. Chaloupka, M. M. Sala, V. Hinkov, M. Haverkort, M. Minola, M. Bakr, K. J. Zhou, S. Blanco-Canosa, C. Monney, Y. T. Song, G. L. Sun, C. T. Lin, G. M. D. Luca, M. Salluzzo, G. Khaliullin, T. Schmitt, L. Braicovic, and B. Keimer, *Nature Phys.* **7**, 725 (2011).
- <sup>4</sup> R. R. P. Singh and M. P. Gelfand, *Phys. Rev. B* **52**, 15695 (1995).
- <sup>5</sup> W. Zheng, J. Oitmaa, and C. J. Hamer, *Phys. Rev. B* **71**, 184440 (2005).
- <sup>6</sup> A. W. Sandvik and R. R. P. Singh, *Phys. Rev. Lett.* **86**, 528 (2001).
- <sup>7</sup> J. Igarashi, *Phys. Rev. Lett.* **46**, 10763 (1992).
- <sup>8</sup> C. J. Hamer, W. Zheng, and P. Arndt, *Phys. Rev. B* **46**, 6276 (1992).
- <sup>9</sup> J. Igarashi and T. Nagao, *Phys. Rev. B* **72**, 014403 (2005).
- <sup>10</sup> A. V. Syromyatnikov, *J. Phys. C* **22**, 216003 (2010).
- <sup>11</sup> H. M. Rønnow, D. F. McMorrow, R. Coldea, A. Harrison, I. D. Youngson, T. G. Perring, G. Aeppli, O. Syljuåsen, K. Lefmann, and C. Rischel, *Phys. Rev. Lett.* **87**, 037202 (2001).
- <sup>12</sup> N. B. Christensen, D. F. McMorrow, H. M. Rønnow, A. Harrison, T. G. Perring, and R. Coldea, *J. Mag. Mag. Mat.* **272-276**, 896 (2004).
- <sup>13</sup> N. B. Christensen, H. M. Rønnow, D. F. McMorrow, A. Harrison, T. G. Perring, M. Enderle, R. Coldea, L. P. Regnault, and G. Aeppli, *Proc. Nat. Acad. Sciences* **104**, 15264 (2007).
- <sup>14</sup> N. S. Headings, S. M. Hayden, R. Coldea, and T. G. Perring, *Phys. Rev. Lett.* **105**, 247001 (2010).
- <sup>15</sup> C. Knetter, K. P. Schmidt, M. Grüninger, and G. S. Uhrig, *Phys. Rev. Lett.* **87**, 167204 (2001).
- <sup>16</sup> K. P. Schmidt and G. S. Uhrig, *Mod. Phys. Lett. B* **19**, 1179 (2005).
- <sup>17</sup> C. Knetter and G. S. Uhrig, *Eur. Phys. J. B* **13**, 209 (2000).
- <sup>18</sup> S. Trebst, H. Monien, C. J. Hamer, Z. Weihong, and R. R. P. Singh, *Phys. Rev. Lett.* **85**, 4373 (2000).
- <sup>19</sup> P. M. Stevenson, *Phys. Rev. D* **23**, 2916 (1981).
- <sup>20</sup> S. Dusuel and G. S. Uhrig, *J. Phys. A: Math. Gen.* **37**, 9275 (2004).
- <sup>21</sup> F. J. Dyson, *Phys. Rev.* **102**, 1217 (1956).
- <sup>22</sup> F. J. Dyson, *Phys. Rev.* **102**, 1230 (1956).
- <sup>23</sup> S. V. Maleev, *Zh. Eksp. Teor. Fiz.* **33**, 1010 (1957).
- <sup>24</sup> S. V. Maleev, *Sov. Phys. JETP* **6**, 776 (1958).
- <sup>25</sup> A. W. Sandvik, *Phys. Rev. B* **56**, 11678 (1997).
- <sup>26</sup> H. Krull, N. A. Drescher, and G. S. Uhrig, *Phys. Rev. B* **86**, 125113 (2012).